OPEN ACCESS
JOURNAL OF ADVANCED DIELECTRICS
Vol. 11, No. 4 (2021) 2150017 (6 pages)

DOI: 10.1142/S2010135X2150017X

Preparation and performance analysis of Pt-IPMC for driving bionic tulip

Aifen Tian*,¶, Xixi Wang*, Yue Sun*, Xinrong Zhang†,
Hongyan Wang‡ and Liang Yang*,§

*College of Materials Science and Engineering
Xi'an University of Science and Technology
Xi'an 710054, P. R. China

†The Key Laboratory of Road Construction Technology and Equipment
MOE, Chang' an University, Xi'an 710064, P. R. China

‡Shaanxi Kekong Technology Industry Research Institute Co. Ltd.
Shaanxi Science and Technology Holding Group
Xi'an 710000, P. R. China

§College of Mechanical Engineering
Xi'an Jiaotong University, Xi'an 710049, P. R. China

¶taf@xust.edu.cn

Received 22 April 2021; Revised 3 June 2021; Accepted 8 June 2021; Published 26 July 2021

Based on the biological characteristics of tulip, the low driving voltage and fast response of ionic polymer metal composite (IPMC), we analyzed the fabrication, morphology and performance of the platinum IPMC (Pt-IPMC) and selected the right IPMC for driving bionic tulip. The preparation and performance of IPMC was analyzed first in this paper such as blocking force, output displacement and bending angle of IPMC under the different directed current voltage (DC). The optimal IPMC sample size and driving voltage were selected based on tulip blooming angles and the strain energy density of IPMC, which completed the blooming process of bionic tulip. The feasibility of IPMC used in driving bionic field was fully proved in this paper, which laid a foundation for the application of IPMC in driving biomimetic biological robots.

Keywords: Bionic tulip; IPMC; intelligent drive; artificial muscle.

1. Introduction

After long-term selection of species in nature, the natural creatures were highly rational, scientific and progressive in information processing, execution and autonomous learning.[1,2] Nowadays, people try to get inspiration from the successful examples in nature to solve human being's problems, so bionic robot was invented.[3] "Bionic robot" refers to a robot system that could imitate the external shape or part functions of species in nature. Nowadays, a lot of researches have been done on bionic robots at home and abroad. For example, the Software Robot Laboratory of the Okayama University in Japan had successively completed two types of soft robots with silicone material and pneumatic drive mode: small-sized flexible manipulator and worm-like autonomous robot.[4,5] Octobot (the first fully software robot) was independently invented by the Bionic Robot Laboratory of the Harvard University.[6] The pneumatic honeycomb network software actuator was invented by Chen Xiaoping's team.[7] Wang liquan *et al*. invented amphibious bionic robot crab[8] and Guo Chuangqiang *et al*. invented the robotic fish.[9] All of the researches have caused great impact on the field of robot. The structure and power source of biology are usually made of "soft materials". Compared with traditional hard intelligent materials,[10,11] soft materials possess the characteristics such as light weight, low cost, easy deformation and better biological affinity and so on, and their deformation ability and driving force are close to biological muscle.[12] Besides the electric driving characteristics,[13,14] IPMC was also used as sensor by experts in the soft robot.[15–17]

Based on the shape and blooming of tulip, we designed and prepared Pt-IPMC to drive its blooming. We studied and analyzed the morphology, structure and performance of the Pt-IPMC and completed the blooming process of bionic tulip. The surface and cross-section morphology of IPMC were observed by JSM-6390A scanning electron microscope (SEM). The blocking force and output displacement of IPMC were observed and analyzed by using DC power generator and coordinate paper. Based on the blooming angles

¶Corresponding author.

of tulip and the strain energy density of IPMC, we selected the optimal size and driving voltage for IPMC to complete the blooming process of bionic tulip, which provided the new idea and direction for the development of bionic industry.

2. Structure Design of Bionic Tulip

Tulip, one of the monocotyledon plants, has conical or cylindrical shape; it usually has 3–5 petals with 50–70 mm long and 20–40 mm wide in strip or lanceolate shape; its petals are usually red or yellow. We observed carefully the characteristics of tulip blooming in nature.[18] Figure 1 shows the blooming time dependencies of the blooming angle of tulip, which uses the method of taking points from the screenshot, so as to design the relevant parameters of bionic tulip. The results show that the full bloom time for tulip was 26 s, and the blooming angle changed little and slowly with the time before 23 s, then changed greatly and quickly, reaching the maximum value of 22 ° at last.

Figure 2 shows the bionic tulip which is composed of petals, receptacle and stems: A is the petal made by hand kneading paper. B, placed between two pieces of hand kneaded paper, is the IPMC actuator, which is used to actuate the bionic tulip. C is the flower holder made by 3D printing, which is used to fix the petals and guide wire together with plastic screw D. E is the simulated green tape used to fix the wire. F is the wire with the diameter of 0.45 mm and used to connect circuit.

3. Preparation of IPMC

IPMC is a sandwich structure material, which is composed of Nafion 117 membrane and noble metal electrode layer on both sides of the membrane. When the voltage is applied

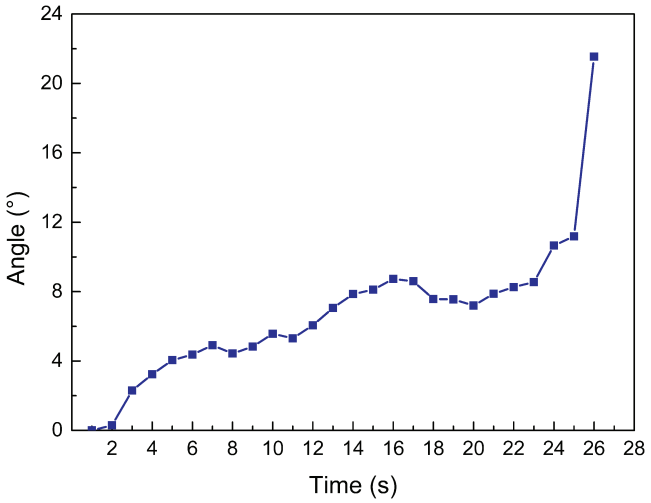

Fig. 1. Blooming times dependencies of the blooming angle of tulip.

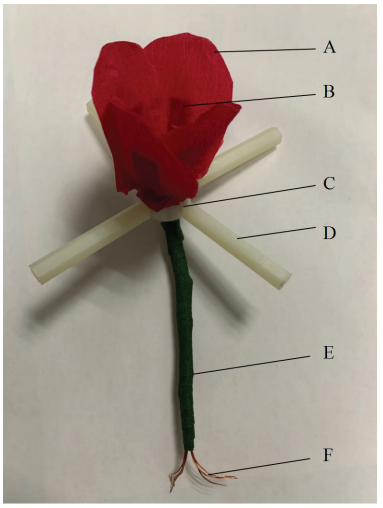

Fig. 2. Structure of bionic tulip.

to both sides of the IPMC, the mobile cation in the Nafion membrane will drag the water molecules to move towards the cathode. The uneven distribution of water molecules in the membrane will lead to the cathode expansion, which is caused the macroscopic bending to the anode.[19,20] In this paper, we used the IPMC's bending characteristics to prepare bionic tulip robot.

3.1. *Materials*

Hydrochloric acid (HCl), ammonia water ($NH_3 \cdot H_2O$), platinum ammonia complex ($[Pt(NH_3)_4]Cl_2$), sodium borohydride ($NaBH_4$), hydrazine hydrate ($N_2H_4 \cdot H_2O$), hydroxylamine hydrochloride ($NH_2OH \cdot HCl$), lithium chloride monohydrate ($LiCl \cdot H_2O$) were obtained from Tianjin Chemical Reagent Corp (Tianjin, China). Nafion-117 membranes with the thickness of 183 μm were obtained from DuPon (Shanghai, China).

3.2. *Testing*

As shown in Fig. 3, the actuation process of IPMC was videotaped by video fixed-point method using DC power generator and coordinate paper. The tip output displacement and bending angle was recorded with a camera under a voltage stimulus of 1–7 V. The electronic balance was used to measure the mass of the specimen with a precision of 0.0001 g, and which could be converted into the blocking force of IPMC. The clamping part length of IPMC was 5 mm (along the length of the sample), and the test point was the end of IPMC. All measurements were performed at room temperature.

3.3. *Definition of IPMC size*

IPMC size was determined by the size range of tulip petals as: length: 30 mm, 40 mm and 50 mm, width: 5 mm and 10 mm.

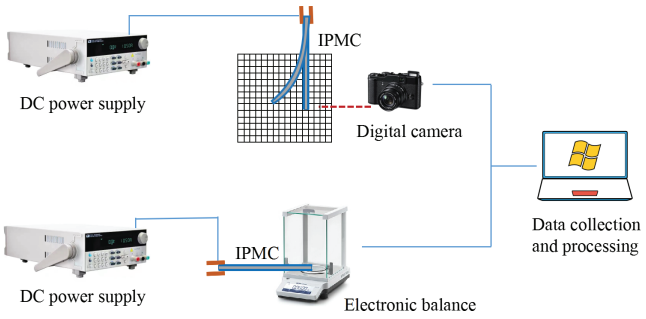

Fig. 3. Schematic diagram of the testing platform of the output displacement and blocking force of IPMC.

According to the principle of permutation and combination, the dimensions of IPMC (length × width) are determined as: 30 mm × 5 mm, 30 mm × 10 mm, 40 mm × 5 mm, 40 mm × 10 mm, 50 mm × 5 mm and 50 mm × 10 mm.

3.4. *Fabrication process*

The fabrication[21,22] of IPMC by chemical reduction method mainly includes the pretreatment of substrate membrane, ion exchange, impregnation-reduction plating (IRP), autocatalytic plating (ACP) and post-treatment (as shown in Fig. 4).

4. Analysis of Morphology and Properties

4.1. *Micromorphology analysis*

Figure 5 shows the surface and section morphology of IPMC. It can be seen from Fig. 5(a) that platinum is relatively dense deposited on the surface of the membrane. The visible concave gullies to the naked eye are caused by grinding. The purpose of grinding is to make platinum deposition on the membrane easily, so the surface of the roughened substrate membrane is not smooth. After the

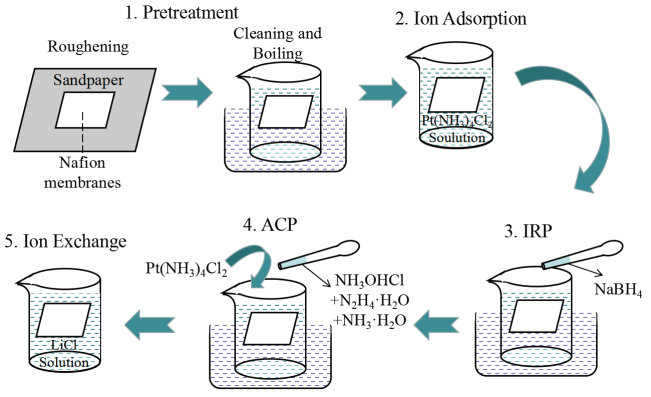

Fig. 4. Fabrication process of Pt-IPMC.

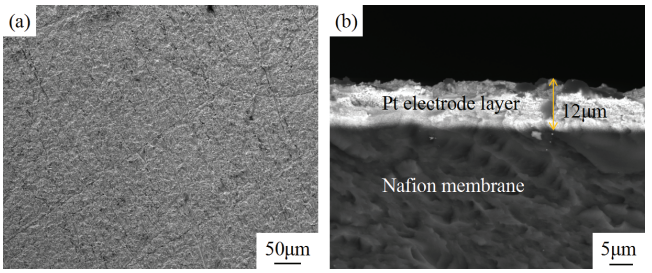

Fig. 5. SEM images of Pt-IPMC with surface (a) and section (b).

deposition of platinum, the surface of the membrane may be concave or convex. The thickness of platinum electrode is about 12 μm, as shown in Fig. 5(b).

4.2. *Actuation performance*

4.2.1. *Output displacement*

Figure 6 shows the output displacement of IPMC with different sizes at different DC voltages. It can be seen from the figure that the output displacement of IPMC increases firstly then decreases with the voltage. The transfer ability of hydrate cation in IPMC increases with voltage's increasing, which means that the output displacement is also increasing. However, the water electrolysis reaction is intensified and the migration of hydrate cations reaches saturation state with continuing increasing voltage, so the output displacement is not increasing any more. Among six Pt-IPMC samples with different sizes, the 50 mm × 5 mm IPMC reaches the maximum output displacement value of 51.43 mm at 5 V. The longer the sample's length, the larger the output displacement for the same width sample. When

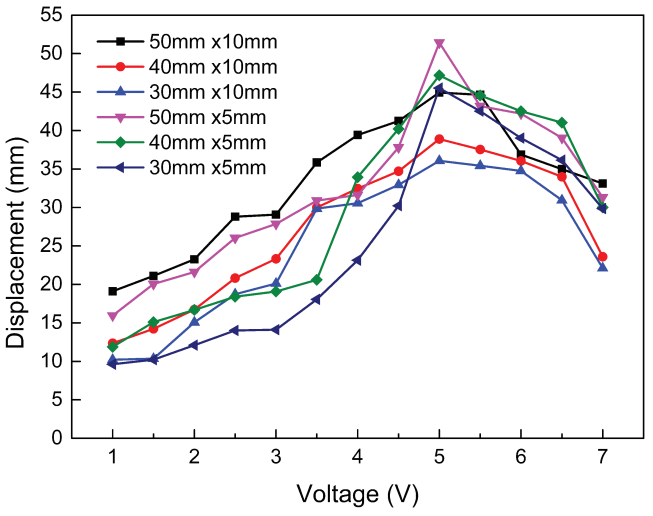

Fig. 6. Output displacement of IPMC with different sizes at different DC voltages.

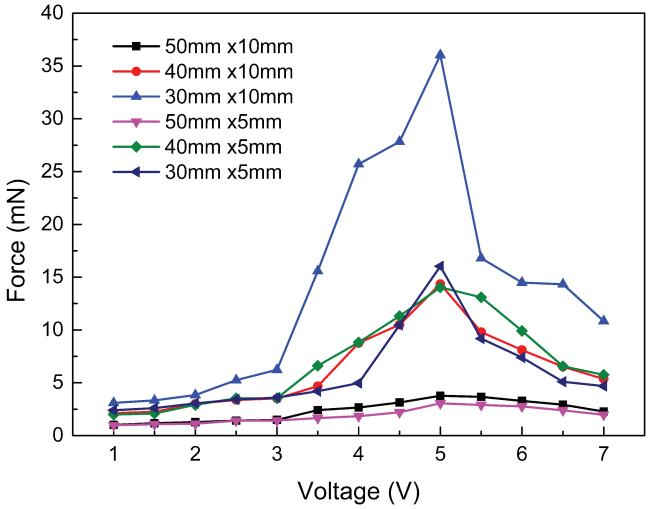

Fig. 7. Blocking force of IPMC with different sizes at different DC voltages.

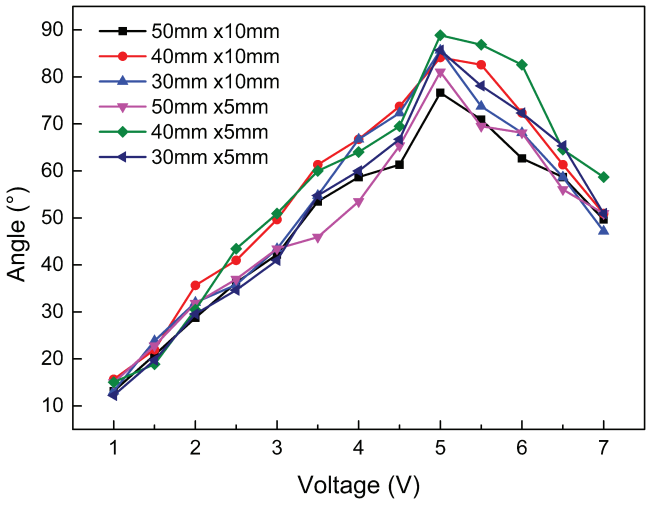

Fig. 8. Bending angle of IPMC with different sizes at different DC voltages.

the length is same, the output displacement of IPMC with 5 mm width is larger than the IPMC with 10 mm.

4.2.2. *Blocking force*

Figure 7 shows the blocking force of IPMC with different sizes at different DC voltages. It can be seen from the figure that the blocking force of IPMC increases first then decreases with the voltage. When the voltage is applied, all the hydrate cations in the IPMC move towards the cathode, giving rise to the difference in concentration, causing the bending of the IPMC. The maximum blocking force value of 36.03 mN at 5 V is obtained in the 30 mm × 10 mm IPMC sample. The shorter the sample's length, the larger the blocking force for the same width.

4.2.3. *Bending angle*

Figure 8 shows the bending angle of IPMC with different sizes at different DC voltages. The bending angle of IPMC is tested so as to select the suitable voltage that fits the maximum blooming angle of tulip. According to bending angle characteristics of tulip (see Fig. 1, the largest angle is 22°), six IPMCs with different sizes are most consistent with the tulip at 1.5 V DC voltage.

4.2.4. *Strain energy density assessment*

According to Figs. 6 and 7, when the output force reaches the maximum, the corresponding output displacement will not reach the maximum in one same sample. Therefore, in order to describe the electro actuation effect of different sizes of IPMC more accurately, the concept of "strain energy density" is specially used. After the voltage is applied to the IPMC, the strain generated in the deformation process of IPMC is composed of shear strain and bending strain. Because the former is far less than the latter, the shear strain can be ignored. According to the bending strain and the Euler–Bernoulli beam theory, it can be seen that[23]

$$\rho_{\varepsilon} = \frac{Flb}{ah(d^2 + b^2)}. \tag{1}$$

Among them: ρ_{ε} is the strain energy density of IPMC, F is the blocking force, l is the length of IPMC sample, b is the output displacement, a is the width, h is the thickness, d is the distance from the test point to the clamping endpoint.

The bending angle of IPMC at 1.5 V DC voltage is the most suitable for the maximum blooming angle of tulip from Fig. 8. Therefore, the strain energy density is carried out at 1.5 V DC voltage. The results calculated according to Eq. (1) are shown in Fig. 9. It can be seen from Fig. 9 that the strain

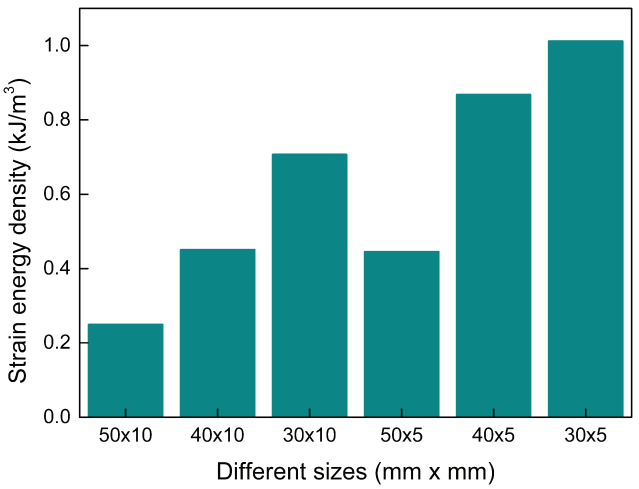

Fig. 9. Strain energy density of IPMC with different sizes at 1.5 V DC voltage.

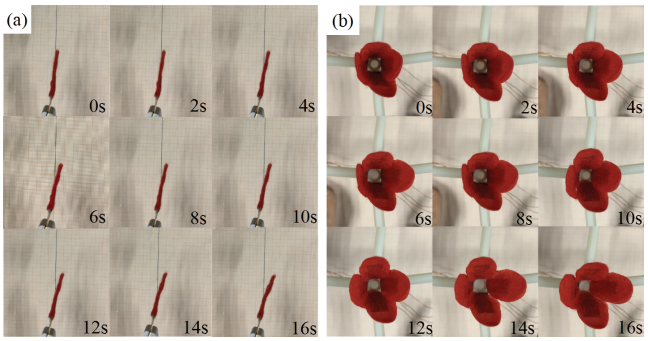

Fig. 10. Driving effect of single petal (a) and four petals (b) at 1.5V DC voltage.

energy density of IPMC with the size of 30 mm × 5 mm is the largest, which is 1.01 kJ/m^3. Therefore, IPMC with this size can be selected as the petal drive material of bionic tulip.

5. Blooming Process of Bionic Tulip

Figure 10(a) shows the opening process of a single petal with 30 mm × 5 mm IPMC at 1.5 V DC voltage. It can be seen from the figure that the single petal starts to bloom slowly at 0 s and reaches the maximum blooming angle at 16 s. Figure 10(b) shows the opening process of four petals. It can be seen from the figure that when four petals are connected in parallel at 1.5 V DC voltage, the IPMC sample will produce four different bending effects, which completely presents the blooming process of bionic tulip from 0 s to 16 s.

6. Conclusion

The Pt-IPMC samples with different sizes were successfully prepared by electroless plating. The results showed that the bending angle, output displacement and blocking force of the six different sizes IPMCs respectively reached the maximum value at 5 V DC voltage. According to the characteristics of blooming angle of tulip and bending angle of Pt-IPMC, six IPMCs with different sizes showed the most consistent with tulip at 1.5 V DC voltage. The 30 mm × 5 mm IPMC sample was used as the actuator to drive the petals of bionic tulip by analyzing the strain energy density. The blooming process of bionic tulip under the controlling of DC voltage was successfully realized in this article. These results provided experimental basis for further realizing the continuous blooming process of bionic plants and laid a foundation for the application of IPMC in driving biomimetic biological robots.

Acknowledgments

The authors acknowledge the financial assistance from the Key Laboratory Project of Expressway Construction Machinery of Shaanxi Province, China (300102259510) and the Key Research and Development Program of Shaanxi Province, China (2018ZDXM-GY-088).

References

[1]Y. Q. Qiu, Z. X. Wang, K. Wang, J. Y. Zhou and K. Feng, Research progress and development trend of bionic robot, *IoT Technol.* **8**, 16 (2016).
[2]H. Y. Xu, Y .L. Fu, S. G. Wang and J. G. Liu, Research on bionic robot, *Robot* **26**, 3 (2004).
[3]A. H. Ji, Z. D. Dai and L. S. Zhou, Research progress of bionic robot, *Robot* **27**, 3 (2005).
[4]K. Suzumori, Flexible microactuator: 1st report, static characteristics of 3 DOF actuator, *Trans. Jpn. Soc. Mech. Eng. Ser. C*. **55**, 518 (1989).
[5]K. Suzumori, Flexible microactuator: 2nd report, dynamic characteristics of 3 DOF actuator, *Trans. Jpn. Soc. Mech. Eng. Ser. C* **56**, 527 (1990).
[6]M. Wehner, R. L. Truby, D. J. Fitzgerald, B. Mosadegh, G. M. Whitesides, J. A. Lewis and R. J. Wood, An integrated design and fabrication strategy for entirely soft, autonomous robots, *Nature* **536**, 7617 (2016).
[7]N. Y. Wang, H. Sun, H. Jiang, X. P. Chen and H. C. Zhang, On grasp strategy of honeycomb pneunets soft gripper, *Robot* **38**, 3 (2016).
[8]L. Q. Wang, L. Sun, D. L. Chen, L. Zhang and Q. X. Meng, Research on prototype of bionic robot crab, *J. Harbin Eng. Univ*. **26**, 5 (2010).
[9]C. Q. Guo, C. Y. Wu and H. Liu, Application progress of ionic polymer metal composites actuator in robots, *J. Mech. Eng*. **53**, 9 (2017).
[10]M. Arshad, H. L. Du, M. S. Javed and A. Maqsood, Fabrication, structure, and frequency-dependent electrical and dielectric properties of Sr-doped $BaTiO_3$ ceramics, *Ceram. Int.* **46**, 2 (2020).
[11]H. L. Du, C. Y. Ma, W. X. Ma and H. T. Wang, Microstructure evolution and dielectric properties of Ce-doped $SrBi_4Ti_4O_{15}$ ceramics synthesized via glycine-nitrate process, *Process. Appl. Ceram*. **12**, 4 (2018).
[12]Y. Xiao, J. P. Wang, X. K. Jiang, X. F. Li and Z. G. Liu, Design and Realization of bionic eight-legged spider robot, *Mechatronics* **12**, 6 (2010).
[13]M. Shahinpoor, Conceptual design, kinematics and dynamics of swimming robotic structures using ionic polymeric gel mugclcs, *Smart Mater. Struct*. **1**, 1 (1992).
[14]K. Sadeghipour, R. Salomon and S. Neogi, Development of a novel electrochemically active membrane and smart material based vibration sensor/damper, *Smart Mater. Struct*. **1**, 2 (1992).
[15]M. Gudarzi, P. Smolinski and W. Qingming, Bending mode ionic polymer-metal composite (IPMC) pressure sensors, *Measurement* **103**, 250 (2017).
[16]W. Jiaqi, M. Andrew, S. Rajnish and C. A. Kean, A compact ionic polymer-metal composite (IPMC) system with inductive sensor for closed loop feedback, *Actuators* **4**, 2 (2015).
[17]L. F. Bian, Z. Jiao and J. H. Liu, Research progress of ion-polymer artificial muscle materials, *Sens. World* **7**, 11 (2001).
[18]Hengshui No. 2 Middle School: Time lapse photography of 2018 campus tulip, Tencent video (2018), https://v.qq.com/x/page/h0616agk491.html?ptag=qqbrowser.
[19]K. Jung, J. Nam and H. Choi, Investigations on actuation characteristics of IPMC artificial muscle actuator, *Sens. Actuators* **107**, 2 (2003).
[20]K. J. Kim and M. Shahinpoor, Ionic polymer-metal composites: II. Manufacturing techniques, *Smart Mater. Struct*. **12**, 1 (2003).

[21]X. Hui, A. F. Tian, Q. Q. Wang, L. Yang, X. R. Zhang and S. S. Cui, Research on process optimization of Ag-IPMC, *Integr. Ferroelectr*. **210**, 106 (2020).
[22]S. Maryam, N. Leila, T. B. Richard and A. T. Faramarz, The enhancement effect of lithium ions on actuation performance of ionic liquid-based IPMC soft actuators, *Polymer* **76**, 140 (2015).
[23]Y. Du, G. Z. Wang, Z. X. Li, B. Liang, P. Zhang, G. Zhao, J. T. Zhao, W. H. Wang, J. Q. Liu and H. Z. Ma, Preparation and characteristic of porous Nafion membrane ionic polymer metal composites, *Polym. Mater. Sci. Eng*. **35**, 7 (2019).